

International Journal of Engineering Research and Development

DOI: 10.29137/ijerad.1756063



Review Article

Ductility Assessment of Hybrid FRP-Steel RC Beams Using Analytical Modeling

Saruhan Kartal^{1*}, Yasin Çağlar ¹

¹Department of Civil Engineering, Faculty of Engineering and Natural Sciences, Kırıkkale University, 71451 Kırıkkale, TÜRKİYE

Final Version: 30/11/2025

Abstract

This study aims to identify the most appropriate ductility definition for hybrid reinforced concrete (RC) beams combining fiber-reinforced polymer (FRP) and steel reinforcement. Although FRP bars are increasingly used due to their high corrosion resistance and tensile strength, their brittle failure mechanism limits ductility, which is critical for structural safety, especially under seismic or overload conditions. Hybrid reinforcement (FRP+steel), integrating the ductility of steel with the durability of FRP, has been proposed to mitigate this limitation. Nevertheless, hybrid systems remain partly susceptible to corrosion due to the presence of steel reinforcement. However, the literature lacks consensus on a standardised ductility definition suitable for such hybrid systems. An extensive experimental dataset of hybrid, FRP-only, and steel-only RC beams was analyzed using multiple ductility definitions from the previous experimental studies to address this gap. Among these, the energy-based definition provided the most consistent and realistic representation of ductile behavior, capturing the elastic-brittle nature of FRP and the yielding response of steel. The selected definition was then extended to additional hybrid RC beams reported in the literature to assess its broader applicability. The analysis confirmed that the ratio of steel reinforcement to total tensile reinforcement (A_s/A_{tot}) significantly influences ductility. A higher A_s/A_{tot} ratio and existence of FRP and steel in the same tensile layer consistently yielded more favorable ductile responses.

Keywords

Ductility, hybrid beams, reinforced concrete, fiber reinforced polymer.

^{*} Corresponding Author: saruhankartal@kku.edu.tr

1. Introduction

Corrosion of reinforcing steel significantly shortens the service life span of RC structures and leads to a substantial increase in maintenance and repair costs. In response to this challenge, FRP bars have emerged as a promising alternative due to their high corrosion resistance and tensile strength. As a result, the application of FRP reinforcement—particularly in flexural members—has gained considerable attention in recent years. Recent research on FRP-reinforced members, addressing both flexural and shear behavior, continues to gain significant attention. Kartal (2024) proposed a new expression for predicting the shear capacity of FRP RC beams without stirrups. Furthermore, Kartal et al. (2025) highlighted that FRP bars cannot be bent and emphasized that the use of prefabricated stirrups at adequate spacing enables RC beams to achieve their flexural capacities. However, despite these advantages, FRP bars also present notable drawbacks. Their modulus of elasticity is significantly lower than that of steel, which imposes limitations in serviceability design. Moreover, FRP exhibits a brittle failure mode, characterized by a linear stress—strain response and sudden rupture at relatively low strain levels. Consequently, the most critical issue in FRP-reinforced elements is their lack of ductility. To ensure sufficient serviceability and to promote more ductile behavior, several design guidelines (e.g., ACI 440.1R-15, 2015; ISIS, 2007) recommend the use of over-reinforced sections in FRP-RC members.

Given the limitations associated with FRP reinforcement, one alternative proposed in the literature is the fabrication of hybrid reinforcement by wrapping FRP fibers around conventional steel bars (Dönmez and Başaran, 2021). However, previous studies have consistently highlighted that employing hybrid reinforced beams, which combine both FRP and steel reinforcement in the tensile region, represents one of the most effective approaches to enhance flexural performance and ductility. Therefore, the present study adopts this widely recommended strategy to ensure both structural efficiency and practical applicability. The main goal of this configuration is to exploit the beneficial properties of both materials while minimizing their respective disadvantages. Specifically, the superior durability and tensile strength of FRP bars are integrated with the ductility and high elastic modulus of steel reinforcement, aiming to produce structural members with enhanced mechanical performance. Several recent studies have explored this concept, demonstrating that hybrid reinforcement can offer a viable solution for achieving both strength and serviceability requirements in aggressive environmental conditions.

Previous studies on hybrid RC beams have primarily focused on load capacity, failure modes, cracking behavior, and deformation characteristics (Aiello and Ombres, 2002; Leung and Balendran, 2003; Qu et al., 2009; Lau and Pam, 2010; Kara et al., 2015; Ge et al., 2015; Refai et al., 2015; Bencardino et al., 2016; Pang et al., 2016; Qin et al., 2017). However, the issue of ductility has received comparatively less attention. Moreover, the majority of these studies have concentrated on over-reinforced hybrid beams, in which the concrete crushes before the FRP reinforcement ruptures. This design approach is primarily based on the assumption that FRP failure is more brittle and thus less desirable than concrete crushing. Nevertheless, this assumption does not constitute a strict requirement for hybrid beams, as they can be designed either as under-reinforced or over-reinforced, depending on the intended behavior. In fact, when properly designed, hybrid beams—regardless of the reinforcement ratio—can allow the steel reinforcement to yield prior to ultimate failure. This yielding behavior facilitates the development of desirable or at least partial ductility before reaching the ultimate load-carrying capacity.

At this scope, although numerous studies have examined the behavior of hybrid RC beams, a clear consensus on an appropriate definition of ductility for such members has yet to be established. Conflicting approaches have been adopted across the literature, and the evaluation of ductility remains inconsistent. In particular, most existing research relies on conventional ductility definitions originally developed for steel-reinforced members, without thoroughly assessing their validity for hybrid systems that combine materials with fundamentally different mechanical responses. This approach has resulted in inconsistent and sometimes contradictory interpretations of ductile behavior. Moreover, the effects of key parameters—such as the ratio of steel reinforcement to total tensile reinforcement (A_s/A_{tot}), the relative placement of FRP and steel within the tensile zone, and the resulting failure mechanisms—have not been systematically investigated in relation to ductility. To address these unresolved issues, the present study employs a comprehensive experimental dataset reported by Kartal et. al. (2023), consisting of 25 RC beams tested under flexure—17 with hybrid reinforcement, 3 with steel-only reinforcement, and 5 with FRP-only reinforcement. This dataset was specifically selected due to the comparable flexural capacities of the specimens, which provides an ideal basis for a consistent evaluation of ductility.

By examining beams with different failure modes and FRP reinforcement types under similar flexural demands, multiple ductility definitions are assessed to determine the most suitable one for hybrid reinforced beams. Based on the selected definition, the study also estimates the ductility levels, flexural capacities, and failure modes of various hybrid beams reported in the literature. Building upon this analysis, the study extends the proposed definition to a broader range of experimental data reported in the literature and conducts a quantitative assessment of how critical design parameters govern the ductile response of hybrid RC beams. In doing so, this research aims to provide a definite understanding of ductility in hybrid reinforced beams and offer a unified framework for future experimental and analytical studies.

Symbols and Abbreviations

RC Reinforced concrete
FRP Fiber reinforced polymer
BFRP Basalt fiber reinforced polymer

	102101D, (2023) 17(3), 337-333, Miriti & Çuğini
GFRP	Glass fiber reinforced polymer
A_s	Cross sectional area of steel reinforcement
A_{tot}	Cross sectional area of total reinforcement
μ	Ductility
δ_{y}	Deformation value at yielding point
δ_{u}	Deformation value at ultimate point
Δ_1	Deformation value at first cracking point
$\Delta_{ m cr}$	Deformation value at first cracking point
E_{tot}	Total energy dissipation capacity
E_{v}	Energy dissipation capacity at yielding point
$M_{\rm u}$	Ultimate moment value
M_{cr}	First cracking moment value
$E_{s(L/180)}$	Energy dissipation capacity at service limit level
U_{H}	Energy dissipation capacity of hybrid beam
U_{S}	Energy dissipation capacity of equivalent steel RC beam
ϕ_{uh}	Ultimate curvature value of hybrid beam
ϕ_{yh}	Yielding curvature value of hybrid beam
E _e	Elastic energy dissipation capacity
S1	Initial slope of moment-curvature curve
S2	Second slope of moment-curvature curve
S3	Third slope of moment-curvature curve
S	Weighted average of the slopes of moment-curvature/load-displacement curve
P1	First cracking load
P2	Yielding load
P3	Maximum load
M1	First cracking moment
M2	Yielding moment
M3	Maximum moment
A_{cs}	Cross sectional area of compression reinforcement
A_{frp}	Cross sectional area of FRP reinforcement
b	Beam width
h	Beam height
L	Beam length
f_c	compressive strength of concrete
f_y	yield strength of steel reinforcement
$f_{\mathrm{fu}}^{'}$	tensile strength of FRP reinforcement
-	last the officer of the control of t

Modulus of elasticity of the FRP reinforcement

2. Method

 E_{f}

2.1. Experimental database

The experimental dataset employed in this study was obtained from Kartal et al. (2023), in which four-point bending tests were conducted on 25 RC beams. These beams were divided into three groups based on their load-carrying capacities and failure modes, with a particular focus on the type of FRP reinforcement used. Each group included beams reinforced solely with steel, solely with FRP, as well as hybrid beams combining BFRP + steel and/or GFRP + steel in the tension zone. The naming convention for the specimens reflects the type and number of longitudinal reinforcement bars placed in the tensile region. The capital letters B, G, and S represent BFRP, GFRP, and steel reinforcement, respectively, while the numbers following each letter indicate the quantity of bars used in that zone.

All beams were tested under two-point loading. Moreover, all beams had adequate shear capacity and reached their load-carrying capacity through flexural failure. The steel-only beams exhibited typical ductile failure. Among the beams reinforced with only FRP, reference specimens B5, G5, G3, and G6 were classified as over-reinforced, where concrete crushing occurred prior to FRP rupture. In the hybrid beams, yielding of the steel reinforcement was observed prior to failure in all specimens, resulting in two distinct flexural failure modes: Under-reinforced failure (URF), in which the FRP bars ruptured before the onset of concrete crushing, and over-reinforced failure (ORF), in which concrete crushing occurred before FRP rupture.

The dataset includes detailed information on reinforcement configurations, concrete compressive strength, mechanical properties of FRP bars, failure modes, and experimentally measured load capacities for all beam specimens (Table 1). The yield strength of the 12 mm diameter steel bars was reported as 470 MPa.

2.2. Analytical Study

In the present study, the main objective regarding hybrid RC beams is to identify the most appropriate definition of ductility. Accordingly, ductility was evaluated using several different definitions. These definitions require theoretical moment—curvature curves for a comprehensive assessment. To obtain the theoretical moment—curvature responses of the hybrid RC beams, an analytical study was conducted. For this purpose, the Todeschini model (1964) was adopted to represent the behavior of concrete. For steel reinforcement, an elasto—plastic model, neglecting strain hardening, was used. The behavior of FRP reinforcement was modeled using linear elastic constitutive models, consistent with its brittle nature.

The moment-curvature curves were obtained by making some assumptions: i. neglecting the contribution of concrete in the tension zone, ii. the plane sections before bending remain plane after bending, iii. the concrete and reinforcement at the same level have the same strain value (full bond acceptance between the concrete and reinforcement). Fig. 1 illustrates the moment—curvature responses of beams categorized based on the type of FRP reinforcement and their corresponding flexural capacities. The results clearly indicate that, within each group, beams reinforced solely with steel and those reinforced solely with FRP exhibit the highest and lowest stiffness values, respectively. In hybrid-reinforced beams, yielding is observed prior to reaching the ultimate load-carrying capacity, and the yielding load level is found to be directly proportional to the amount of steel reinforcement present in the tensile zone. Moreover, the curvature capacity of hybrid-reinforced beams exhibits a noticeable increasing trend with higher proportions of FRP reinforcement, which is characterized by a relatively lower modulus of elasticity.

Table 1. Details, mechanical properties, flexural failure modes and load capacity of the test beams

		Sectional		Concrete	FRP	FRP	Flexural	Load	
Group	Specimen	Dimensions	Tension Reinforcement	Strength	(GPa)	Tensile	Failure	Capacity	
		(mm)		(MPa)	(Gi a)	Str. (MPa)	Mode	(kN)	
	S5 REFERENCE	200x300	5φ12 Steel	31.28	=	=	URF	125.02	
	B1S4	200x300	1φ8.68 BFRP + 4φ12 Steel	31.28	43	1034	URF	122.26	
	B2S3	200x300	2φ8.68 BFRP + 3φ12 Steel	31.28	43	1034	ORF	116.64	
	B3S2	200x300	3φ8.68 BFRP + 2φ12 Steel	31.28	43	1034	ORF	116.59	
	B4S1	200x300	4φ8.68 BFRP + 1φ12 Steel	31.28	43	1034	ORF	123.56	
1 st	B5 REFERENCE	200x300	5φ8.68 BFRP	31.28	43	1034	ORF	120.75	
	G184	200x300	1φ12.86 GFRP + 4φ12 Steel	31.28	35	449	URF	129.72	
	G2S3	200x300	2φ12.86 GFRP + 3φ12 Steel	31.28	35	449	ORF	130.90	
	G3S2	200x300	3φ12.86 GFRP + 2φ12 Steel	31.28	35	449	ORF	130.22	
	G4S1	200x300	4φ12.86 GFRP + 1φ12 Steel	31.28	35	449	ORF	128.20	
	G5 REFERENCE	200x300	5φ12.86 GFRP	31.28	35	449	ORF	141.11	
	S6 REFERENCE	199.8x303.29	6φ12 Steel	30.49	-	-	URF	146.26	
	G1S5	200.8x301.86	1φ12.23 GFRP + 5φ12 Steel	30.49	46	580	ORF	135.98	
	G2S4	199.8x301.14	2φ12.23 GFRP + 4φ12 Steel	30.49	46	580	ORF	141.04	
2 nd	G3S3	200.6x304.43	3φ12.23 GFRP + 3φ12 Steel	30.49	46	580	ORF	153.57	
	G4S2	198.6x304.57	4φ12.23 GFRP + 2φ12 Steel	30.49	46	580	ORF	154.95	
	G581	200.6x306.00	5φ12.23 GFRP + 1φ12 Steel	30.49	46	580	ORF	149.80	
	G6 REFERENCE	200.0x307.00	6φ12.23 GFRP	30.49	46	580	ORF	147.56	
III.	S3 REFERENCE	200.8x304.71	3φ12 Steel	30.49	-	-	URF	84.16	
	B1S2	199.8x308.00	1φ8.68 BFRP + 2φ12 Steel	30.49	43	1034	ORF	83.82	
3 rd	B2S1	199.2x301.71	2φ8.68 BFRP + 1φ12 Steel	30.49	43	1034	URF	79.14	
3	G1S2	198.6x304.86	1φ12.23 GFRP + 2φ12 Steel	30.49	46	580	URF	85.32	
	G2S1	202.0x301.57	2φ12.23 GFRP + 1φ12 Steel	30.49	46	580	URF	101.25	
	G3 REFERENCE	198.8x308.71	3φ12.23 GFRP	30.49	46	580	ORF	114.96	

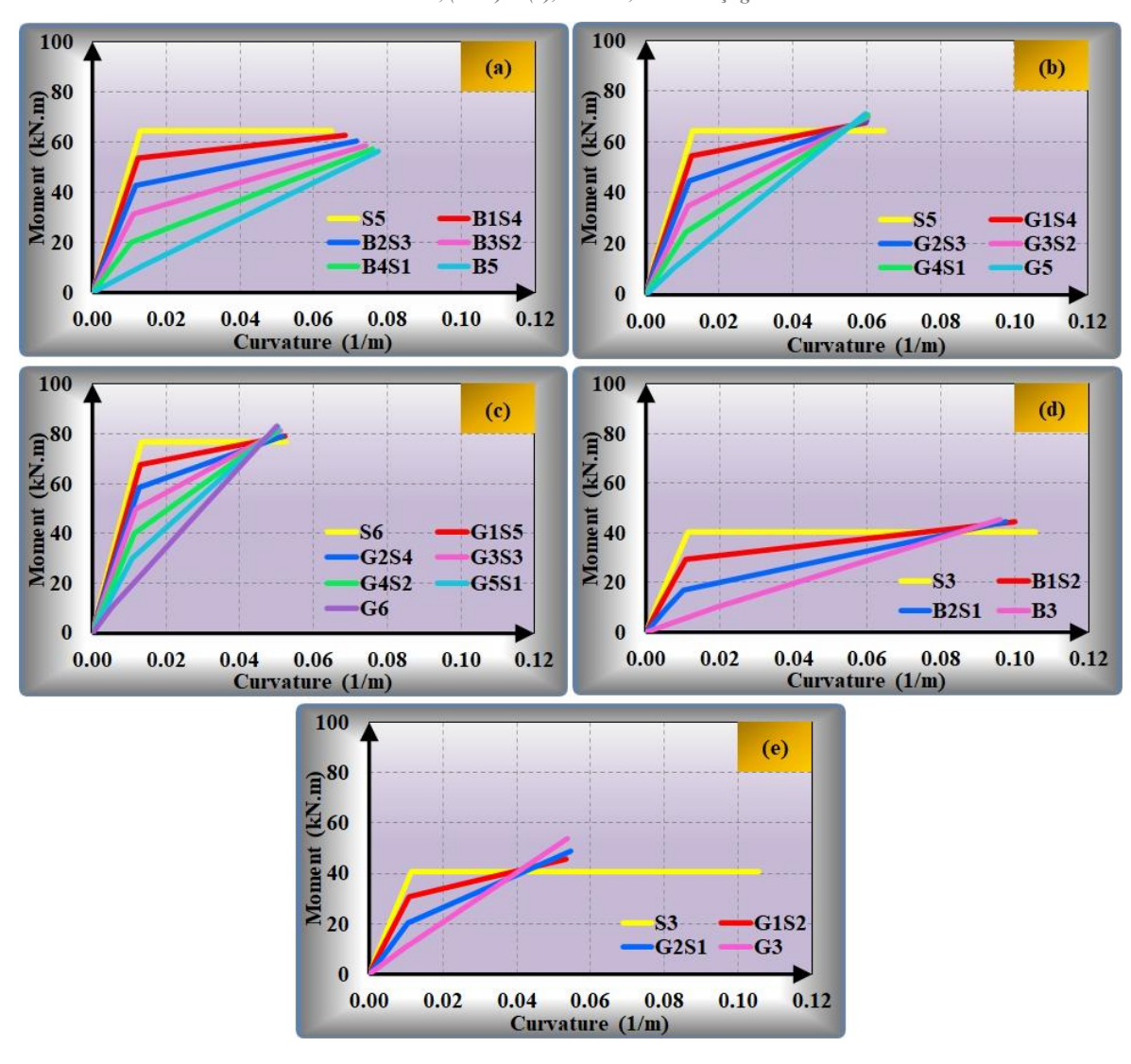


Fig. 1 The moment curvature curves of the (a) first group beams with BFRP-steel reinforcement; (b) first group beams with GFRP-steel reinforcement; (c) second group beams; (d) third group beams with BFRP-steel reinforcement; (e) third group of beams with GFRP-steel reinforcement

2.3. Evaluation of ductility

2.3.1. Classical deformation ductility definition

As the ratio of FRP to total reinforcement in hybrid reinforced beams increases, the yielding of steel reinforcement occurs at lower load levels and the deformability of the beams increases due to the relatively low modulus of elasticity of FRP reinforcement. For these reasons, using the classical deformation ductility definition (Eq. 1) causes unrealistic results in hybrid RC beams. According to this definition, while the beams with a high proportion of FRP reinforcement, which is a brittle material, are more ductile, the beams with only steel reinforcement are the ones with the lowest ductility value. However, hybrid RC beams were a design method that was developed in order to prevent the non-ductile behavior of FRP RC beams. Therefore, the classical deformation ductility definition (Eurocode 2, 2004) is not suitable for hybrid FRP-steel reinforced beams, but a deformability definition.

$$\mu = \frac{\delta_u}{\delta_y} \tag{1}$$

 δ_y and δ_u symbolize the deformation values at the point where the yielding and the maximum load drop to 85%, respectively. According to Eq.1, ductility values for each experimental group are presented in Fig. 2. As illustrated in Fig. 2, when the classical definition of ductility is applied to hybrid beams, the highest ductility values are observed in specimens with the largest proportion of FRP reinforcement, even though FRP exhibits an inherently brittle material behavior. This observation suggests that conventional ductility metrics may lead to misleading interpretations when directly applied to hybrid systems.

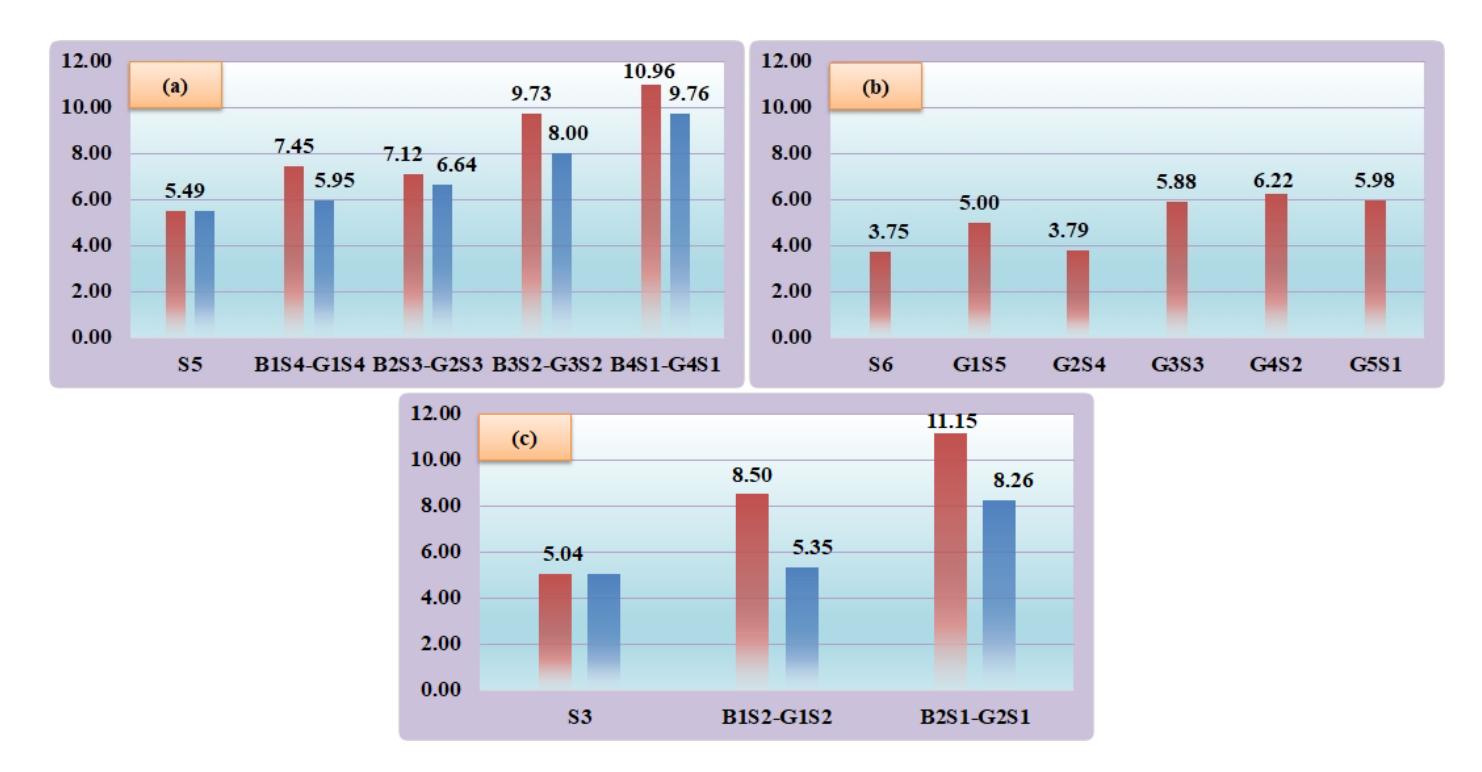


Fig. 2 The ductility values of the beams according to classical deformation ductility definition

2.3.2. Abdelrahman et. al. (1996) Ductility Definition

Abdelrahman et al. (1996) proposed a new ductility definition for prestressed T-section bridge beams with FRP tendons. Since FRP tendons do not show yielding characteristic property and remain elastic until beams reach bending capacity, they adopted the idea that nonlinear behavior in the beams starts with cracking of concrete. The ductility definition was expressed as in Eq. 2, depending on the deformation (Δ_1) that the section would do if it had not cracked.

$$\mu = \frac{\Delta_u}{\Delta_1} \tag{2}$$

 Δ_u shows the ultimate deformation value of the beam. According to this definition, the ductility values of beams were determined with the help of experimental load-deflection curves of the beams and presented in Fig. 3. According to the Fig. 3, relation could not be established between ductility values and reinforcement ratios. This definition was originally proposed for prestressed T-section bridge beams with FRP tendons and does not yield a meaningful correlation when applied to hybrid beams. The fact that specimens S5–B5–G5 exhibit significantly different ductility values, while S3–B3–G3 show nearly identical results, further supports the conclusion that this definition is not suitable for hybrid beams. This definition was originally proposed for prestressed T-section bridge beams with FRP tendons and does not yield a meaningful correlation when applied to hybrid beams. The fact that specimens S5–B5–G5 exhibit significantly different ductility values, while S3–B3–G3 show nearly identical results, further supports the conclusion that this definition is not suitable for hybrid beams.

2.3.3. Spadea et. al. (2001) Ductility definition

Spadea et. al. (2001) evaluated the ductility of steel RC beams strengthened with an externally bonded CFRP laminate using Eq. 3. In the energy-dependent expression of the classical definition of ductility, E_{tot} and E_y represent the energy consumed by the beam until the ultimate and yielding level, respectively.

$$\mu = \frac{E_{tot}}{E_{V}} \tag{3}$$

The ductility values obtained with the help of experimental load-deflection curves of the beams were given in Fig.3 and Fig 4. The ductility definition, like other classical definitions, gives the result that as the FRP reinforcement ratio increases, the ductility generally increase. Thus, this expression is also a deformability definition for hybrid RC beams.

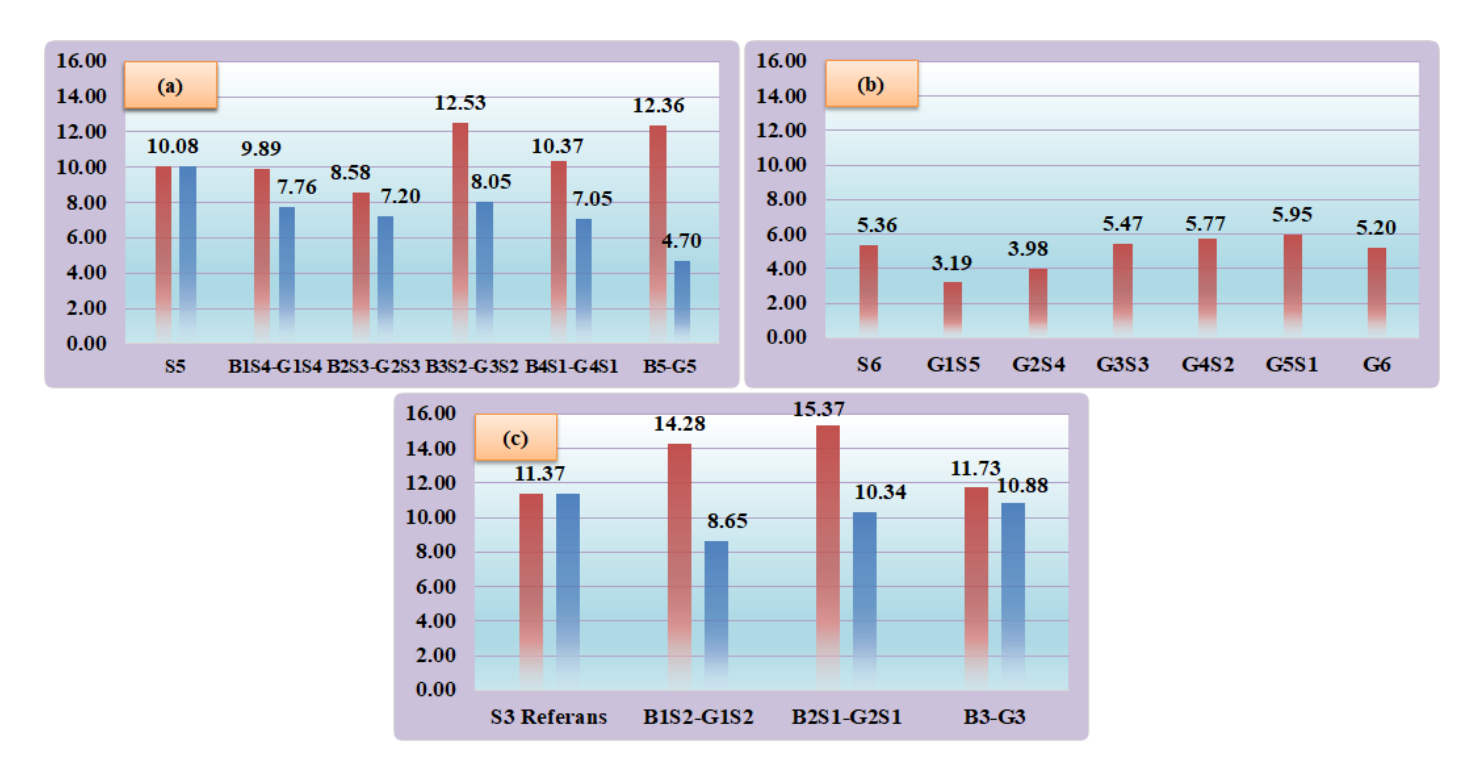


Fig. 3 The ductility values of the beams according to Abdelrahman et. al. (1996) ductility definition

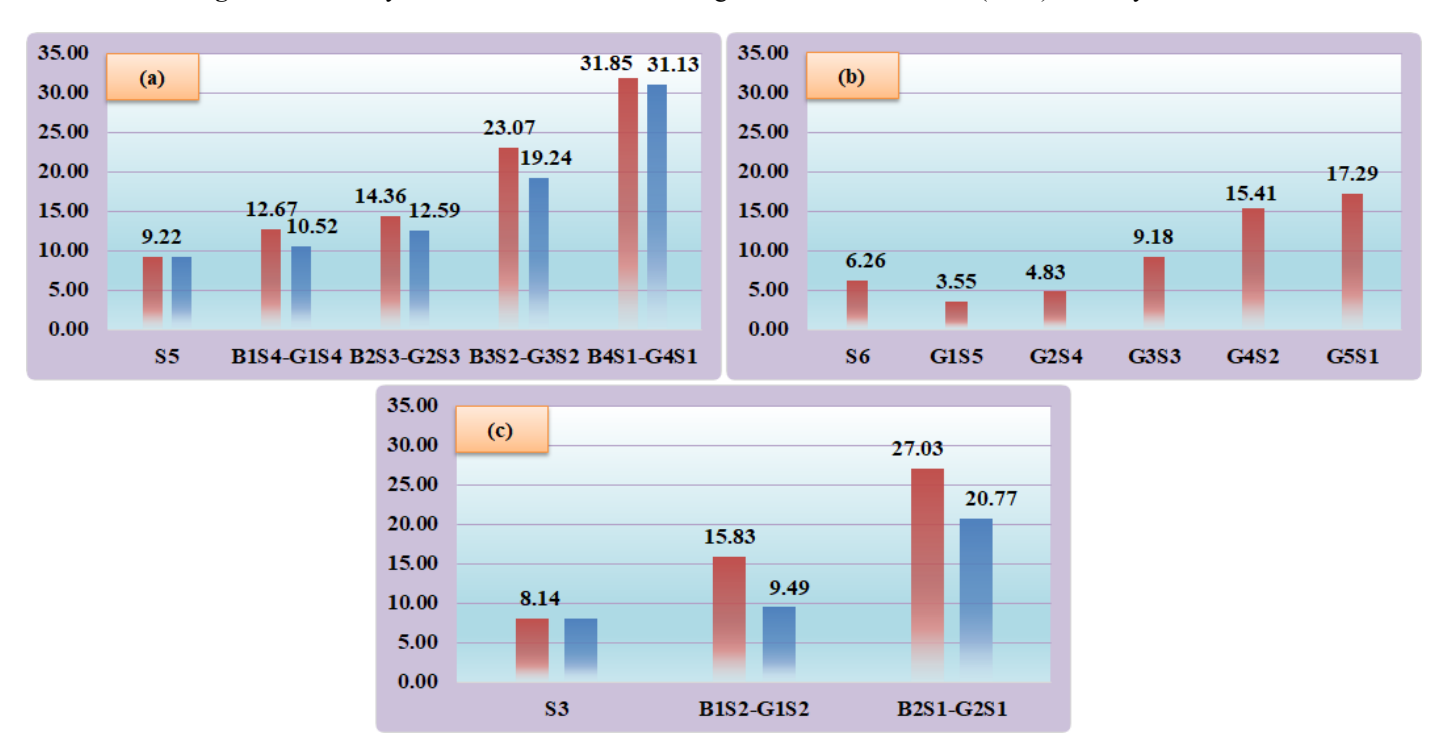


Fig. 4 The ductility values of the beams according to Spadea et. al. (2001) ductility definition

2.3.4. Zou (2003) Ductility Definition

Zou (2003) evaluated the ductility of the steel or FRP tendon beams with a new expression considering the concrete strength (Eq. 4).

$$\mu = \left(\frac{\Delta_u}{\Delta_{cr}}\right) \left(\frac{M_u}{M_{cr}}\right) \tag{4}$$

 Δ_{cr} represents the deflection value corresponding to the first cracking point, while M_{cr} and M_u show the first cracking and ultimate moment value, respectively. The ductility values obtained using the Zou (2003) ductility definition based on the experimental load deformation curves of the beams are given in Fig. 5. Since the direct relationship between the beam ductility values in Fig. 6 and the FRP reinforcement ratio, Zou (2003) definition is also not suitable for hybrid FRP-steel RC beams. In addition, the lowest ductility values belong to only steel RC beams in each specimen group.

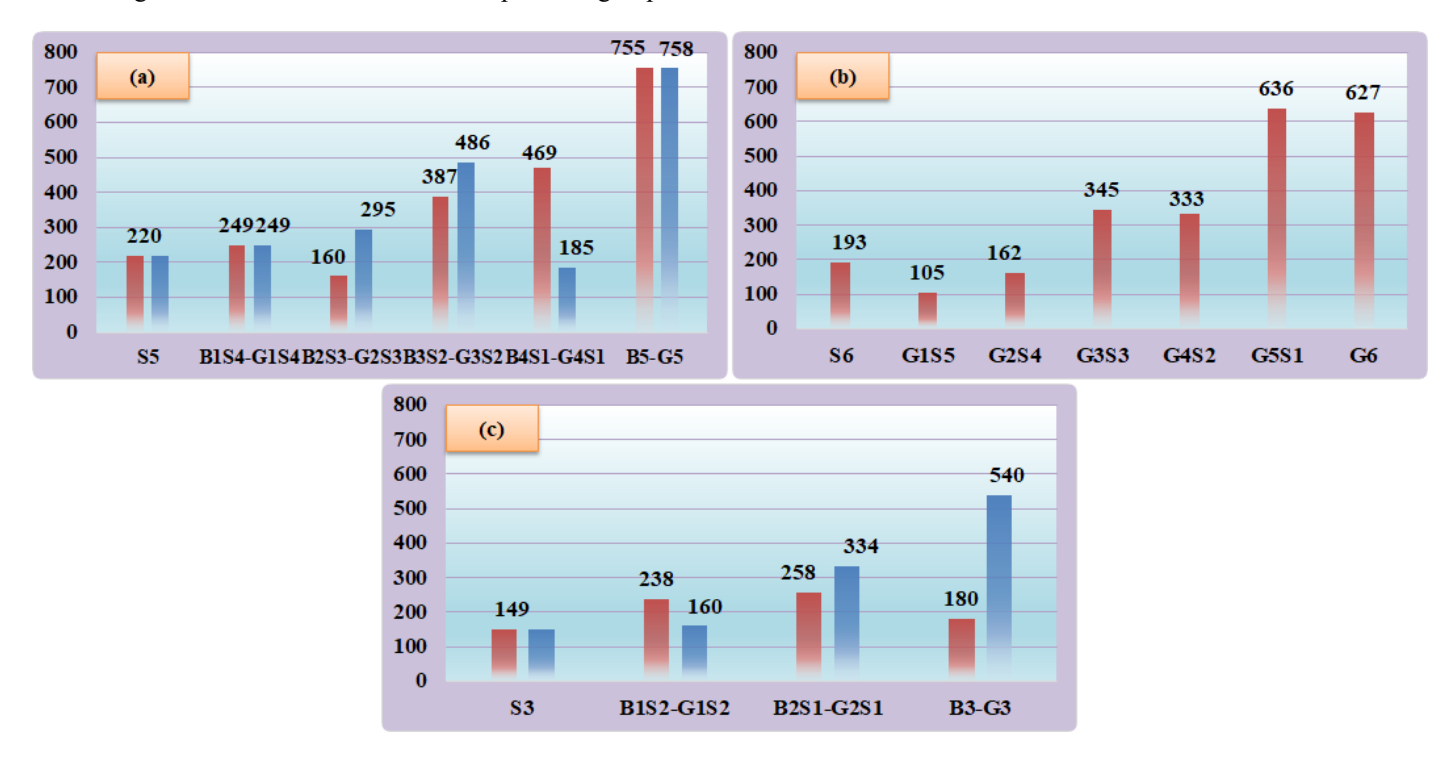


Fig. 5 The ductility values of the beams according to Zou (2003) ductility definition

2.3.5. Vijay ve GangaRao (2001) Ductility Definition

Vijay and GangaRao (2001) evaluated the GFRP RC beams ductility according to a different ductility definition that was was expressed as the ratio of the energy consumed by ultimate to service limit level (Eq. 5). For the service limit level L/180 deformation value was defined. $E_{s(L/180)}$ shows the energy consumed by the beam within the service limit level. In Fig. 6, the ductility values obtained by using experimental load-deflection curves were given.

$$\mu = \frac{E_{tot}}{E_{S(L/180)}} \tag{5}$$

In general, the ductility value of only steel RC beams is the lowest in all specimen groups, and as the FRP reinforcement ratio increases, the beam ductility tends to increase. Therefore, this definition is also a deformability definition for hybrid FRP-steel RC beams.

2.3.6. Lei Pang et. al. (2016) Ductility Definition

Lei Pang et. al. (2016) developed a new ductility expression based on deformability and energy absorption capacity (Eq. 6). In this definition, equivalent steel RC beams were created for each hybrid RC beams in terms of effective steel reinforcement ratio equality $(A_{stl} = A_{st} + A_{frp} \cdot E_f/E_s)$. A_{stl} , shows the steel reinforcement area of the equivalent beam. A_{st} and A_{frp} represent the steel reinforcement and FRP reinforcement respectively. E_f and E_s symbolizes elasticity modulus of FRP and steel reinforcement, respectively.

Moment-curvature diagrams of each hybrid RC beam and its equivalent beam were obtained and the total consumed energy (with the help of the areas under the graphs) was calculated. The new definition includes the reduction of ductility values to realistic level by using an reduction coefficient (ψ) in hybrid reinforced beams. The coefficient was defined as the ratio of the energy consumed by the hybrid RC beam to equivalent steel RC beam (Eq. 7):

$$\mu = \Psi \frac{\varphi_{uh}}{\varphi_{yh}} \tag{6}$$



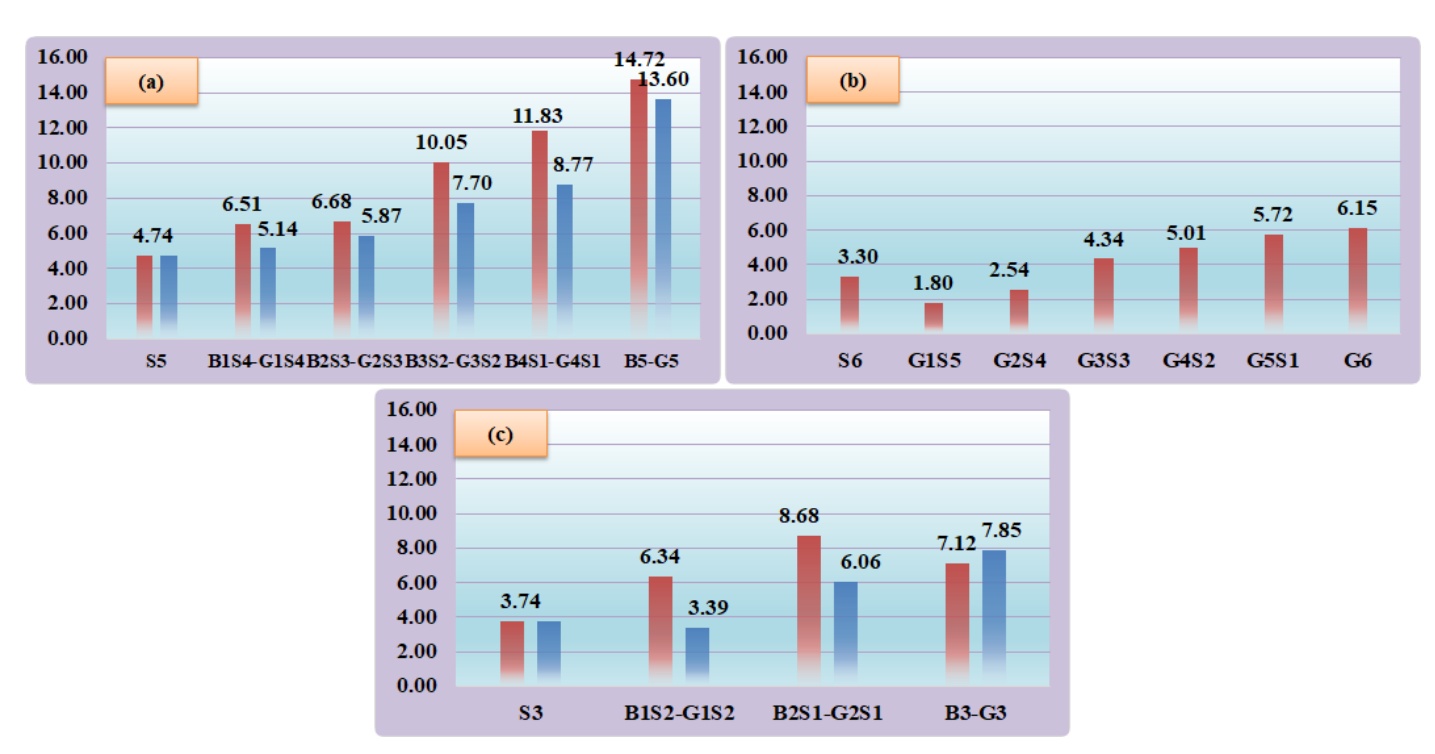


Fig. 6 The ductility values of the beams according to Vijay and GangaRao (2001) ductility definition

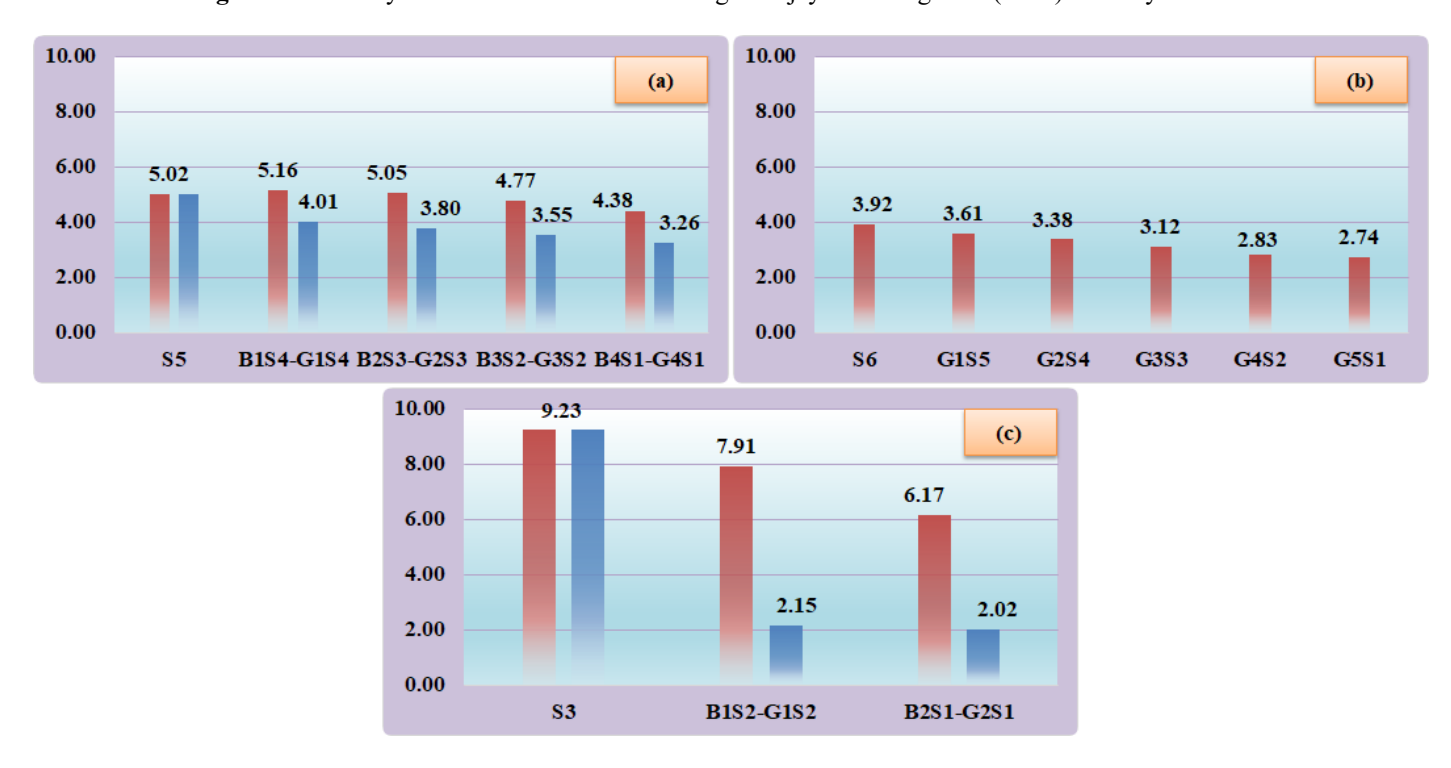


Fig. 7 The ductility values of the beams according to Pang et. al. (2016) ductility definition

The energy absorpiton capacities of hybrid and equivalent steel RC beams are shown with U_H and U_S , respectively. The ultimate and yielding curveture values of the hybrid RC beams are indicated by φ_{uh} and φ_{yh} , respectively. Fig. 7 shows the Pang et. al. (2016) ductility values obtained with the help of theoretical moment curvature diagrams of beams.

Among the ductility definitions evaluated so far, this definition is the most suitable for hybrid RC beams. The highest ductility values in all experimental groups belong only steel RC beams and the ductility values decrease gradually as the ratio of FRP reinforcement increases. The most important disadvantage of this definition is that the ductility reduction coefficient cannot be explained mathematically. Therefore, comparing Lei Pang et. al. (2016) ductility values to code limit ductility values may not give accurate results.

2.3.7. Naaman and Jeong (1995) Ductility Definition

Since FRP tendon or rebar do not have yielding characteristic, classical ductility definitions cannot be used for the beams reinforced with FRP tendon or rebar. In order to evaluate the ductility of these beams, Naaman and Jeong (1995) developed a new definition based on energy. The classical ductility expression ($\mu = \Delta_u / \Delta_y$) was expressed in terms of energy by using the ratio of total (E_{tot}) to elastic energy (E_e) consumed by a steel RC beam (Fig. 8 (a)) which show elasto-plastic behavior (Eq. 8). One of the most important advantages of using this definition is that the ductility values are directly comparable to the classical ductility values.

$$\mu = \frac{1}{2} \left(\frac{E_{tot}}{E_e} + 1 \right) \tag{8}$$

The unloading slope S is obtained by computing the weighted average of the slopes SI and S2 (Eq. 9). The slope SI corresponds to the initial linear response, measured from the beginning of loading up to the point of first cracking. The slope S2, on the other hand, extends from the first cracking point to the point at which concrete loses its elastic behavior. The load levels corresponding to the onset of cracking and the loss of elastic behavior in the concrete are denoted by PI and P2, respectively. Finally, E_e is calculated by using the triangle area, which corresponds to the maximum load (P_{max}) and have a hypotenuse obtained using S slope from that point.



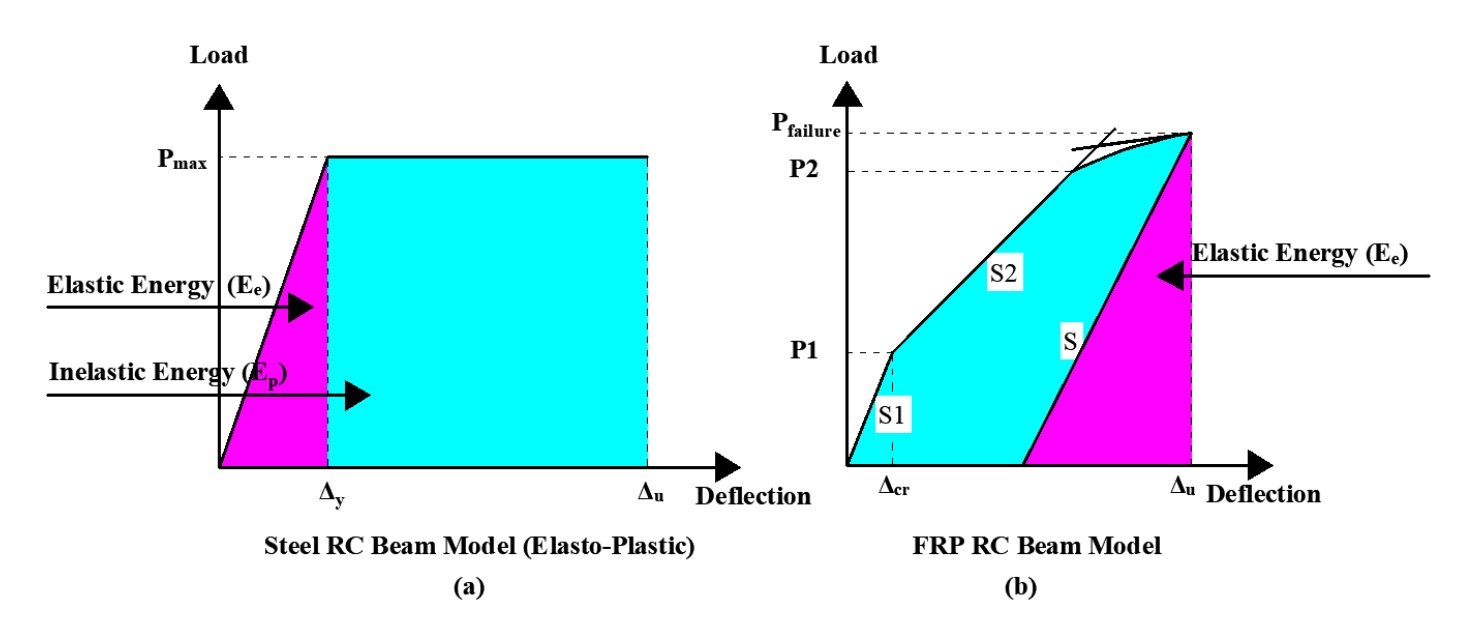


Fig. 8 (a) Steel (b) FRP RC beam load-deflection and energy model

Grace et al. (1998) suggested that the unloading slope S should be calculated as the weighted average of three slopes, including the slope of the region where the concrete loses its elastic behavior. In hybrid reinforced beams, the load—deformation response typically exhibits three linear slopes (Fig. 9 (a)). Moreover, it should be noted that after the yielding of the steel reinforcement, the FRP bars continue to deform elastically, and a portion of the energy absorbed beyond the steel yielding point remains elastic in nature. Therefore, in the present study, the calculation of the unloading slope S based on Eq. 10 was deemed appropriate and consistent with the actual behavior of hybrid RC beams. Using this method, the ductility values can be obtained by converting hybrid reinforced beams to elastoplastic format correctly. In Fig. 9 (b), three different examples are given that show the conversion of moment-curvature curves of the hybrid RC beams to elasto-plastic format.

$$S = \frac{M1 \cdot S1 + (M2 - M1) \cdot S2 + (M3 - M2) \cdot S3}{M3} \tag{10}$$

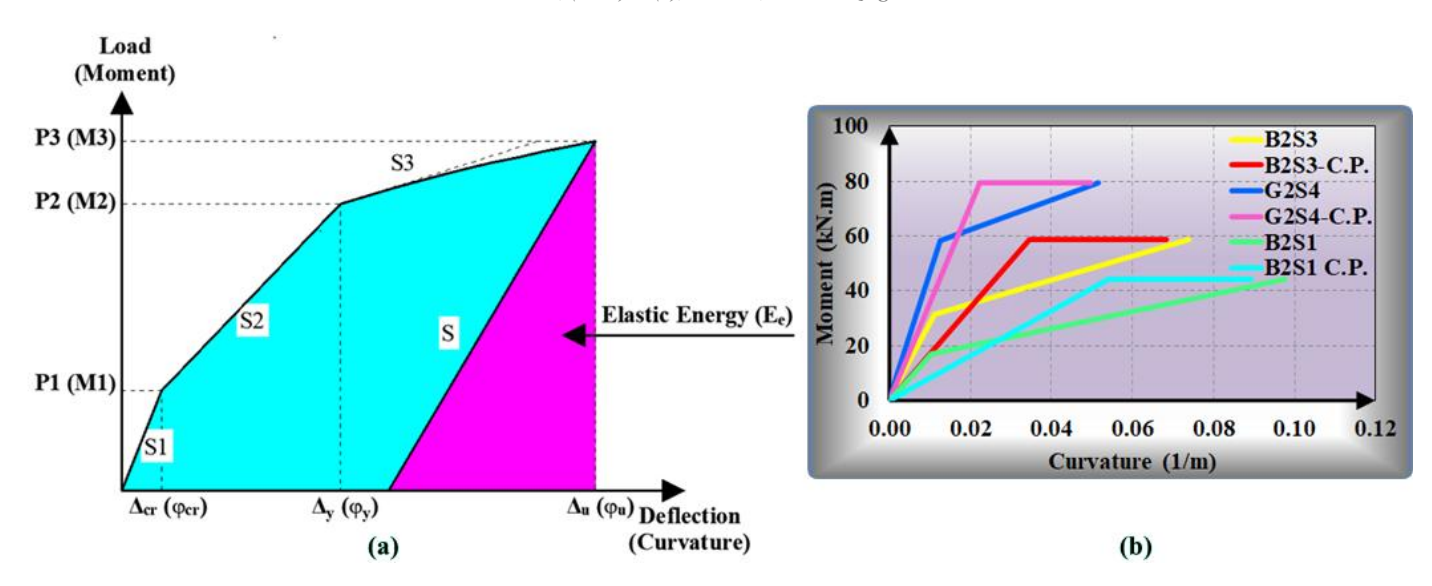


Fig. 9 (a) Hybrid RC beam load-deflection and energy model (b) three different examples showing the conversion of momentcurvature curves of the hybrid RC beams to elasto-plastic format

M1, M2 and M3 are the moment values corresponding to the first cracking, yielding of steel reinforcement and failure, respectively.. Accordingly, Table 2 includes the ductility values of the all group beams and the ratio of the ductility value of the beams to the reference steel RC beam in each group is given in Fig. 10.

The ductility values are normalized with respect to fully steel-reinforced reference beams (S5, S6, and S3 for Groups a, b, and c, respectively), allowing direct comparisons within each group (Fig. 10). In Fig.10 (a), the fully steel-reinforced beam S5 serves as the reference with a normalized ductility of 1.00. Hybrid beams such as B1S4 and G1S4 recorded ductility values of 0.78 and 0.61, respectively, indicating that even a small replacement of steel with FRP leads to a noticeable reduction in ductility. Beams B2S3 and G2S3 exhibited further reductions, down to 0.58 and 0.43, respectively. The trend continues with beams like B3S2 (0.39) and G3S2 (0.31), culminating in the fully FRP-reinforced beams B5 and G5, both with the lowest ductility value of 0.20. These values reflect a progressive loss of ductility as the steel ratio decreases and FRP content increases. A similar trend is observed in Fig.10 (b), where S6 is again the reference at 1.00, followed by the hybrid beams G1S5 (0.73), G2S4 (0.57), and G3S3 (0.44). As the steel content continues to decline, ductility further drops to G4S2 (0.35), G5S1 (0.29), and finally to G6 (0.26) a beam with only GFRP reinforcement, again showing the lowest value.

In Fig. 10 (c), where S3 is the reference beam with 1.00, the hybrid beams B1S2-G1S2 show ductility values of 0.40, while B2S1-G2S1 range between 0.24 and 0.14. The lowest values in this group are found in B3 and G3, both with 0.11, reaffirming the brittle nature of fully FRP-reinforced elements. Additionally, a consistent pattern across all groups is the superior performance of BFRP-hybrid beams compared to GFRP-hybrid beams at similar reinforcement levels. For example, B3S2 (0.39) consistently outperformed G3S2 (0.31), and B1S2 (0.40) was superior to G1S2 (0.40) or G2S1 (0.14), emphasizing the comparatively higher strain capacity or energy absorption potential of BFRP.

The evaluation of ductility in RC beams is essential for understanding their post-elastic behavior and ensuring sufficient deformation capacity under seismic or overload conditions. At the present study, various ductility definitions were applied to a comprehensive set of hybrid, steel-only, and FRP-only reinforced beams. Based on the results, it is evident that the selected definition (Naaman and Jeong, 1995) provides the most accurate and consistent representation of ductility for hybrid RC beams. Beams reinforced solely with FRP exhibited the lowest ductility values, which is expected given the brittle nature of FRP materials. In contrast, steel-reinforced beams demonstrated significantly higher ductility due to the yielding capacity of steel, allowing for considerable plastic deformation before failure. Hybrid RC beams exhibited intermediate ductility values, with a clear trend: as the proportion of FRP reinforcement increased, ductility values decreased gradually, particularly in over-reinforced hybrid beams. Importantly, this ductility definition is consistent with the classical definition of ductility, making the results directly comparable to ductility limits specified in various design codes and standards. This compatibility enhances the practical relevance of the findings and supports their integration into performance-based design approaches for hybrid RC members.

Table 2. The ductility values of the beams according Naaman and Jeong (1995) ductility definition

	Table 2. The ductility values of the beams according Naaman and Jeong (1995) ductility definition											
Group	Beam	M1	M2	M3	S1	S2	S3	S	M_{max}	E_{tot}	E_e	μ
		(kN.m)	(kN.m)	(kN.m)	(kNm^2)	(kNm^2)	(kNm^2)	(kNm^2)	(kN.m)	(kJ)	(kJ)	
	S5	10.67	64.34	64.34	5323.91	4916.78	-	4984.30	64.34	3.75	0.42	5.02
	B1S4	10.67	53.63	62.91	4569.41	4285.01	165.25	3725.42	62.91	3.61	0.53	3.90
	B2S3	10.67	42.66	60.50	3758.29	3570.95	298.43	2638.98	60.50	3.34	0.69	2.91
	B3S2	10.67	31.40	58.72	2877.69	2763.55	435.42	1701.10	58.72	3.01	1.01	1.98
	B4S1	10.67	19.83	57.39	1907.90	1846.44	575.22	1025.93	57.39	2.63	1.61	1.32
1 st	B5	10.67	-	56.36	811.63	-	711.48	730.44	56.36	2.22	2.17	1.01
	G1S4	10.67	54.71	67.49	4647.15	4351.54	270.72	3625.67	67.49	3.23	0.63	3.07
	G2S3	10.67	44.87	68.61	3925.16	3720.34	494.72	2636.00	68.61	2.99	0.89	2.18
	G3S2	10.67	34.80	69.72	3149.36	3016.46	713.85	1883.43	69.72	2.76	1.29	1.57
	G4S1	10.67	24.49	70.62	2307.13	2228.66	932.99	1394.12	70.62	2.48	1.79	1.19
	G5	10.67	-	71.08	1377.72	-	1160.09	1192.75	71.08	2.17	2.12	1.01
	S6	9.95	76.95	76.95	6113.36	5679.20	-	5735.32	76.95	3.53	0.52	3.92
	G1S5	9.90	67.56	79.13	5465.25	5155.14	295.78	4483.59	79.13	3.31	0.70	2.87
	G2S4	9.81	58.23	79.29	4812.82	4597.80	540.75	3546.80	79.29	3.05	0.89	2.22
2^{nd}	G3S3	10.06	49.56	81.26	4273.22	4133.57	809.04	2854.08	81.26	2.86	1.16	1.74
	G4S2	9.97	39.91	81.26	3551.41	3467.68	1057.54	2251.67	81.26	2.60	1.47	1.39
	G5S1	10.17	30.21	82.68	2812.28	2769.86	1325.11	1858.31	82.68	2.40	1.84	1.15
	G6	10.28	-	83.26	1968.36	-	1626.59	1668.77	83.26	2.13	2.08	1.01
	S3	10.40	40.52	40.52	3605.79	3519.92	-	3541.96	40.52	4.05	0.23	9.23
	B1S2	10.47	29.34	44.62	2763.77	2724.18	171.10	1859.33	44.62	3.46	0.54	3.73
	B2S1	9.93	16.94	44.45	1647.46	1635.47	315.25	821.18	44.45	2.77	1.20	1.65
3^{rd}	B3	9.82	-	45.15	511.39	-	460.23	471.36	45.15	2.20	2.16	1.01
	G1S2	9.99	30.66	45.84	2830.24	2785.46	358.00	1991.21	45.84	1.79	0.53	2.20
	G2S1	9.95	20.31	48.96	1941.64	1924.14	650.22	1182.35	48.96	1.63	1.01	1.31
	G3	10.29	-	53.95	1076.02	-	988.34	1005.07	53.95	1.47	1.45	1.01

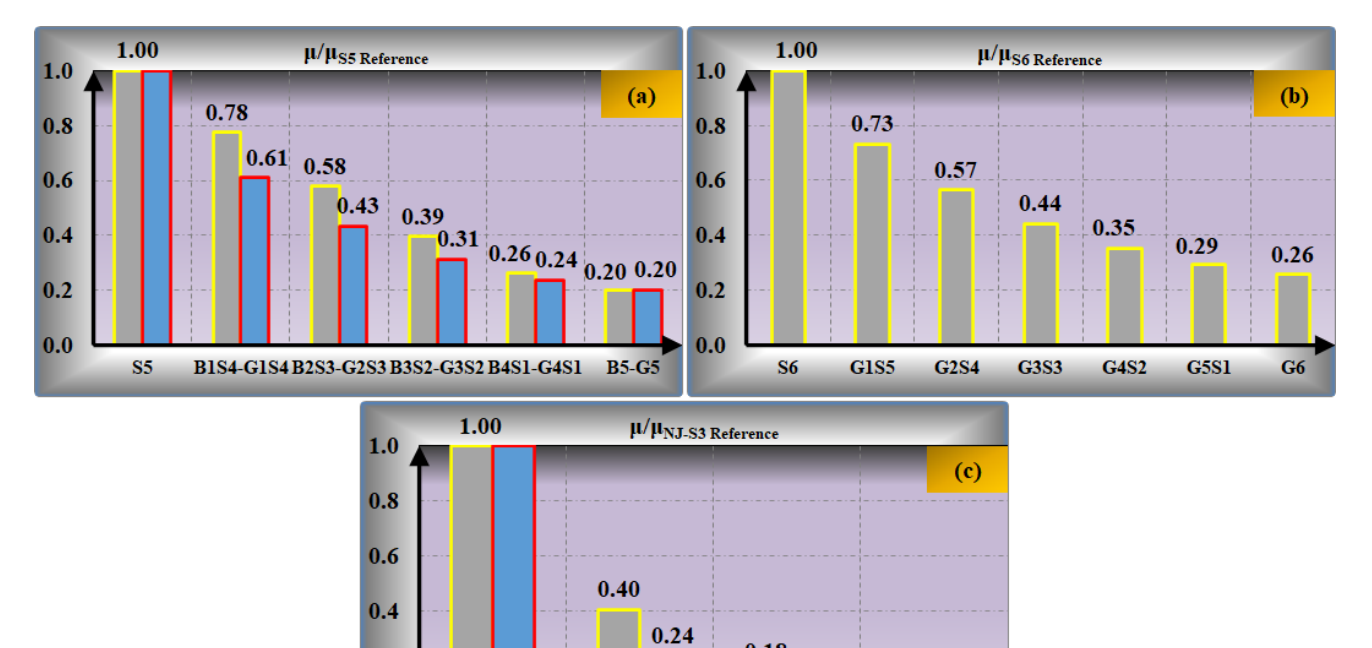


Fig. 10 The ratio of the ductility values of the (a) 1st group (b) 2nd group (c) 3rd group beams to the reference steel RC beam in each group

B1S2-G1S2

0.2

0.0

S3

0.18 0.14

B2S1-G2S1

0.11 0.11

B3-G3

3. Discussion

3.1. Evaluation of ductility based on previous experimental studies

In the preceding sections of this study, a comprehensive evaluation was conducted using an experimental dataset developed by Kartal et al. (2023), which included a total of 25 RC (RC) beams comprising 17 hybrid, 5 only FRP, and 3 only steel specimens tested under four-point bending. The primary objective of this analysis was to identify the most appropriate ductility definition for hybrid RC beams. Various definitions were examined, and it was concluded that the most suitable approach was the one based on the ratio of total energy to elastic energy. This definition not only conforms to the classical concept of ductility, but also explicitly considers the inherently elastic behavior of FRP reinforcement, making it particularly appropriate for systems that incorporate both ductile (steel) and brittle (FRP) materials. The adoption of this energy-based formulation enables a consistent and realistic representation of post-yield behavior in hybrid RC members.

Building upon this framework, the current section extends the scope of the investigation by incorporating additional hybrid RC beams reported in the literature. The aims of this extended analysis are twofold: (1) to examine the robustness and applicability of the selected ductility definition across a wider variety of beam geometries, reinforcement combinations, and experimental conditions; and (2) to identify general behavioral trends that may guide the performance-based design of hybrid RC beams. Within this context, particular attention is given to the ratio of steel reinforcement area to the total tensile reinforcement area (As/Atot), which is considered a key parameter influencing the ductile behavior of hybrid RC beams. In such systems, the post-elastic response is primarily governed by the relative proportions and mechanical interaction of the ductile (steel) and brittle (FRP) reinforcement components. Accordingly, the As/Atot ratio offers a rational and quantifiable basis for evaluating ductility, as it directly reflects the contribution of steel reinforcement within the composite tensile system. By systematically analyzing the relationship between ductility values and this ratio, the study aims to identify consistent behavioral trends and propose threshold values for minimum steel content that ensure sufficient ductility in structural design.

In this context, Table 3 provides comprehensive details for various beams reported in the literature. Using the material models adopted in the analytical study, the ductility values of these beams were calculated based on the selected ductility definition and are also presented in the table. b, h, and L represent the beam's width, height, and length, respectively. A_s , A_{frp} , A_{cs} , and A_{tot} denote the areas of steel reinforcement, FRP reinforcement, compression reinforcement, and total tensile reinforcement, respectively. E_f corresponds to the modulus of elasticity of the FRP reinforcement. Additionally, f_c , f_y , and f_{fu} denote the compressive strength of concrete, the yield strength of steel, and the ultimate tensile strength of FRP reinforcement, respectively. In hybrid beams, a design approach found in the literature involves placing steel reinforcements in the inner layer to enhance corrosion resistance. For beams whose names are marked with a star (*), the FRP and steel reinforcements are not located in the same layer. However, this arrangement reduces the effectiveness of the steel reinforcement and may consequently affect the ductility values. Therefore, in Fig. 11, the cases where FRP and steel reinforcements are used in the same layer and in different layers are considered separately.

Table 3. Details of the other hybrid RC beams reported in the literature and their calculated ductility values

				1 abic			other hyt		- Ucailis			incrature		i caiculau		J						
Study	Beam	b (mm)	h (mm)	L (mm)	A_s (mm^2)	A_{frp} (mm^2)	A_{cs} (mm^2)	f _c (MPa)	f _y (MPa)	f _{fu} (MPa)	E_f (GPa)	M1 (kNm)	M2 (kNm)	M3 (kNm)	S1 (kNm2)	S2 (kNm2)	S3 (kNm2)	S (kNm2)	E_{tot} (kJ)	E _e (kJ)	μ	As/Atot
	A1*	150	200	2700	100.53	88.36	100.53	38.85	465	1674	49.00	4.00	8.10	20.09	354.03	458.23	107.20	227.95	1.65	` ′	1.43	0.53
Aiello and	A2*	150	200	2700	100.53	157.08	100.53	38.85	465	1366	50.10	4.03	9.42	25.82	409.59	496.89	185.39	285.37	1.65			0.39
Ombres (2002)	A3*	150	200	2700	226.19	235.62	100.53	38.85	465	1366	50.10	5.24	17.24	33.74	657.06	978.70	267.71	581.08	1.73			0.49
(2002)	C1	150	200	2700	100.53	88.36	100.53	38.85	465	1674	49.00	4.05	9.17	21.13	468.35	621.03	103.78	299.06	1.82			0.53
Lau and	G0.3-MD1.0	280	380	4200	981.75	283.53	-	41.30	336	588	39.50	30.44	105.69	155.99	11413.57	16519.94	896.49	10485.60				0.78
Pam	G0.6-T1.0	280	380	4200	981.75	567.06	-	44.60	550	588	39.50	31.63	180.74	236.44	11970.10	15856.55	1808.15	12027.23	7.47	2.32	2.11	0.63
(2010)	G1.0-T0.7	280	380	4200	628.32	981.75	-	39.80	597	582	38.00	28.75	147.92	224.14	9672.59	12491.88	2712.07	8804.64	6.11	2.85	1.57	0.39
Loung	H2*	150	200	2200	157.08	142.66	-	48.80	460	760	40.80	4.41	11.05	21.74	355.16	522.24	111.66	286.55	1.69	0.82	1.53	0.52
Leung and	H5*	150	200	2200	157.08	213.99	-	48.80	460	760	40.80	4.39	12.31	24.87	387.31	555.53	157.27	324.70	1.63	0.95	1.35	0.42
Balendran	L2*	150	200	2200	157.08	142.66	-	28.50	460	760	40.80	3.37	10.85	16.55	323.00	452.44	92.29	302.21	0.98	0.45	1.58	0.52
(2003)	L5*	150	200	2200	157.08	213.99	-	28.50	460	760	40.80	3.40	12.09	18.52	351.76	482.90	125.64	334.82	0.94	0.51	1.42	0.42
	В3	180	250	1800	226.19	253.35	-	28.14	363	782	45.00	6.75	20.38	40.44	1414.18	1999.97	360.30	1088.95	1.80	0.75	1.70	0.47
	B4	180	250	1800	201.06	397.11	-	28.14	336	755	41.00	6.73	18.84	43.61	1410.54	2040.66	486.51	1060.72	1.68	0.90	1.44	0.34
Qu et. al.	B5	180	250	1800	402.12	141.76	-	29.24	336	778	37.70	7.26	27.96	39.36	1859.81	2689.71	187.51	1811.63	2.20	0.43	3.07	0.74
(2009)	В6	180	250	1800	402.12	253.35	-	29.24	336	782	45.00	7.21	29.80	46.69	1931.03	2804.59	353.95	1783.27	1.99	0.61	2.13	0.61
	B7	180	250	1800	113.10	141.76	-	34.55	363	778	37.70	7.13	10.42	31.53	869.79	1561.90	209.72	499.93	2.16	0.99	1.59	0.44
	B8*	180	250	1800	1206.36	397.113	-	34.55	336	755	41.00	8.79	73.88	74.37	3669.74	4386.16	25.68	4273.11	2.02	0.65	2.06	0.75
	2G12-1S10	230	300	3700	78.54	226.19	100.53	40.00	520	1000	50.00	13.52	16.19	60.52	1132.03	3488.22	524.92	791.06	3.33	2.31	1.22	0.26
	2G12-2S10	230	300	3700	157.08	226.19	100.53	40.00	520	1000	50.00	13.99	25.18	65.46	1646.60	2334.33	520.40	1071.05	3.66	2.00	1.42	0.41
Refai et.	2G12-2S12	230	300	3700	226.19	226.19	100.53	40.00	520	1000	50.00	14.04	32.93	69.96	2048.92	2739.27	517.30	1424.65	3.89	1.72	1.63	0.50
al. (2015)	2G16-2S10	230	300	3700	157.08	402.12	100.53	40.00	520	1000	50.00	13.95	29.87	80.60	1872.02	2542.75	844.37	1357.80	3.51	2.39	1.23	0.28
	2G16-2S12	230	300	3700	226.19	402.12	100.53	40.00	520	1000	50.00	14.09	37.47	84.49	2240.74	2971.07	837.25	1661.80	3.67	2.15	1.35	0.36
	2G16-2S16	230	300	3700	402.12	402.12	100.53	40.00	520	1000	50.00	14.43	56.29	94.94	3044.61	3995.59	822.22	2559.17	3.96	1.76	1.62	0.50
	2G12-1S16	180	300	1600	201.06	226.19	100.53	30.32	540	868.22	40.06	9.79	30.79	55.09	1853.71	2372.35	428.62	1422.76	2.64	1.07	1.74	0.47
	2G12-2S12 (D)*	180	300	1600	226.19	226.19	100.53	30.32	517	868.22	40.06	9.61	29.31	53.24	1593.36	1994.33	448.87	1227.27	2.42	1.15	1.55	0.50
Ruan et	2G12-2S12	180	300	1600	226.19	226.19	100.53	30.32	517	868.22	40.06	9.87	32.63	56.87	2023.94	2608.03	435.78	1580.61	2.70	1.02	1.82	0.50
al.	2G16-1S16	180	300	1600	201.06	402.12	100.53	30.32	540	958.2	45.69	9.85	36.30	68.85	2103.89	2682.83	778.06	1699.46	2.45		1.38	0.33
	2G16-2S12 (D)*	180	300	1600	226.19	402.12	100.53	30.32	517	958.2	45.69	9.65	34.50	66.17	1817.16	2189.56	814.00	1476.96	2.23			0.36
	2G16-2S12	180	300	1600	226.19	402.12	100.53	30.32	517	958.2	45.69	9.91	37.61	69.79	2230.88	2865.83	776.43	1812.18	2.48			0.36
	B10-6S*	100	200	1220	157.08	56.55	-	30.00	530	780	41	2.36	11.16	13.20	283.14	370.99	44.83	305.05	0.72			0.74
Safan	B10-8S*	100	200	1220	157.08	100.53	-	30.00	530	755	39	2.35	12.08	14.61	301.80	388.56	67.51	319.02	0.69			0.61
(2013)	B12-6S*	100	200	1220	226.19	56.55	-	30.00	470	780	41	2.38	13.22	14.52	331.46	435.59	38.41	382.75	0.67			0.80
	B12-8S*	100	200	1220	226.19	100.53	-	30.00	470	755	39	2.39	14.03	15.68	345.25	448.94	57.81	391.90	0.65			0.69
Ge et. al.	FS1	200	300	2500	314.16	301.59	-	28.10	360	880	55	11.13	35.69	71.76	3145.40	4389.78	825.62	2405.13	2.50			0.51
(2015)	FS2	200	300	2500	392.70	251.33	-	28.10	360	880	55	11.44	41.16	71.56	3476.53	4863.72	696.90	2872.21	2.64			0.61
	FS3	200	300	2500	471.24	201.06	-	28.10	360	880	55	11.54	46.55	71.30	3762.14	5310.20	568.25	3413.44	2.78			0.70
	S1G4	150	300	3000	78.54	519.56	157.08	30.00	420	449	35	8.05	18.17	69.76	1717.80	2127.59	984.76	1235.16	2.38			0.13
Yaz	S2G3	150	300	3000	157.08	389.67	157.08	30.00	420	449	35	8.34	23.83	63.26	2133.17	2627.95	686.35	1352.43	2.61			0.29
(2014)	S3G2	150	300	3000	235.62	259.78	157.08	30.00	420	449	35	8.55	29.38	56.72	2513.75	3089.52	431.69	1721.42	2.87		2.04	0.48
	S4G1	150	300	3000	314.16	129.89	157.08	30.00	420	449	35	8.81	34.82	50.18	2861.95	3520.21	217.31	2393.69	3.18	0.53	3.52	0.71

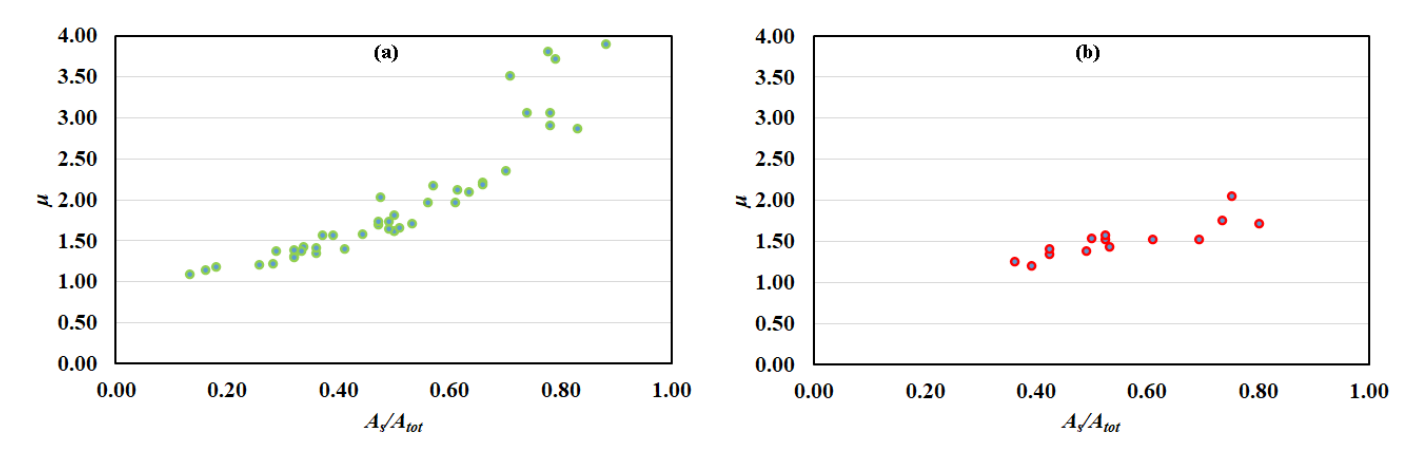


Fig. 11 The ductility values and corresponding A_{st}/A_{tot} ratios in hybrid RC beams with FRP and steel reinforcements (a) same layer (b) different layer

The ductility performance (μ) of hybrid RC beams was evaluated as a function of the ratio of steel reinforcement to total tensile reinforcement (A_s/A_{tot}), considering two distinct reinforcement configurations identified in the literature: (i) where steel and FRP bars are placed within the same tensile layer, and (ii) where steel bars are positioned in an inner layer. The comparative analysis reveals that A_s/A_{tot} is a governing parameter in the ductility behavior of such hybrid systems. Regardless of the configuration, a general trend of increasing ductility with higher A_s/A_{tot} ratios is evident, consistent with findings from Kartal et al. (2023) and other studies in the literature.

In the first configuration (Fig. 11(a)) where steel and FRP are co-located—a strong linear relationship ($R^2 = 0.8195$) was observed between A_s/A_{tot} and ductility. This highlights the critical contribution of ductile steel reinforcement, which yields under tensile loading and provides significant energy dissipation. In contrast, FRP reinforcements exhibit a brittle failure mode, characterized by elastic behavior up to sudden rupture. In the second configuration (Fig. 11(b)) where steel is embedded in an inner layer although a positive correlation remains ($R^2 = 0.7323$). In this case, FRP, owing to its higher stiffness and external position, absorbs most of the tensile demand early in the loading process. This may delay or inhibit the yielding of the steel reinforcement, limiting its beneficial contribution and leading to a more brittle structural response. The trend observed across both configurations supports a broader conclusion in hybrid reinforcement research: an increase in the proportion of steel within the tensile reinforcement generally leads to enhanced ductility, provided that the layout allows for effective engagement of the steel bars. In summary, the results underline the dual importance of both quantity and placement of steel reinforcement in hybrid FRP-steel systems. To effectively counterbalance the brittle nature of FRP and harness the full ductility potential of steel, reinforcement configurations that promote co-located tensile action are preferable. These findings not only reinforce current understanding but also provide practical design insights for improving the deformability and seismic resilience of hybrid RC elements.

4. Conclusion

The current study evaluates, the ductility behavior of hybrid FRP-steel RC beams based on previous experimental studies and various ductility definitions from the literature. Unlike steel only reinforced concrete beams, hybrid beams incorporate both brittle (FRP) and ductile (steel) reinforcement, which complicates the application of classical ductility formulations. Through comprehensive analytical modeling, it was determined that the energy-based ductility definition proposed by Naaman and Jeong (1995) most accurately captures the post-yield behavior of hybrid RC beams. This definition considers both the elastic energy stored in FRP bars and the plastic deformation capacity of steel reinforcement, offering a more realistic and comparable measure of ductility across different reinforcement configurations.

The study further extended the analysis to a wide range of hybrid beams reported in the literature, revealing that the ratio of steel reinforcement to total tensile reinforcement (A_s/A_{tot}) is a key parameter affecting ductility. Beams with higher A_s/A_{tot} ratios, especially when steel and FRP are placed in the same tensile layer, demonstrated improved ductile performance. Conversely, configurations where the steel is positioned in an inner layer were found to limit the effectiveness of the steel contribution, leading to reduced ductility. These findings underscore the importance of both the quantity and placement of steel reinforcement in hybrid RC systems.

5. References

Abdelrahman, A. A., Tadros, G., & Rizkalla, S. H. (1996). Test model for the first Canadian smart highway bridge. ACI Structural Journal, 92(1), 1–10.

ACI Committee 440. (2015). Guide for the design and construction of structural concrete reinforced with fiber-reinforced polymer (FRP) bars (ACI 440.1R-15). American Concrete Institute.

Aiello, M. A., & Ombres, L. (2002). Structural performances of concrete beams with hybrid (fiber-reinforced polymer-steel) reinforcements. Journal of Composites for Construction, 6(2), 133–140. https://doi.org/10.1061/(ASCE)1090-0268(2002)6:2(133)

Bencardino, F., Condello, A., & Ombres, L. (2016). Numerical and analytical modeling of concrete beams with steel, FRP and hybrid FRP-steel reinforcements. Composite Structures, 140, 53–65. https://doi.org/10.1016/j.compstruct.2015.12.045

Comité Européen de Normalisation (CEN). (2004). Eurocode 2: Design of concrete structures – Part 1-1: General rules and rules for buildings (prEN 1992-1-1). European Committee for Standardization.

CSA. (2010). Canadian highway bridge design code (CSA S6-10). Canadian Standards Association.

Dönmez, E. T., & Başaran, B. (2021). Bond Strength of Epoxy Impregnated Carbon Fiber Wrapped Steel Reinforcement. International Journal of Engineering Research and Development, 13(2), 625-634.

El Refai, A., Abed, F., & Al-Rahmani, A. (2015). Structural performance and serviceability of concrete beams reinforced with hybrid (GFRP and steel) bars. Construction and Building Materials, 96, 518–529. https://doi.org/10.1016/j.conbuildmat.2015.08.063

Ge, W., Zhang, J., Cao, D., & Tu, Y. (2015). Flexural behaviors of hybrid concrete beams reinforced with BFRP bars and steel bars. Construction and Building Materials, 87, 28–37. https://doi.org/10.1016/j.conbuildmat.2015.03.113

Grace, N. F., Soliman, A. K., Abdel-Sayed, G., & Saleh, K. R. (1998). Behavior and ductility of simple and continuous FRP reinforced beams. Journal of Composites for Construction, 2(4), 186–194. https://doi.org/10.1061/(ASCE)1090-0268(1998)2:4(186)

ISIS Canada. (2007). Reinforcing concrete structures with fibre-reinforced polymers. Intelligent Sensing for Innovative Structures.

Kara, I. F., Ashour, A. F., & Köroğlu, M. A. (2015). Flexural behavior of hybrid FRP/steel RC beams. Composite Structures, 129, 111–121. https://doi.org/10.1016/j.compstruct.2015.03.073

Kartal, S. (2024). Shear Behaviors of FRP Longitudinally Reinforced Concrete Beams without Stirrups ($\alpha/d > 2.5$). International Journal of Engineering Research & Development (IJERAD), 16(1).

Kartal, S., & Kısıklı, E. (2024). Bending Behavior of RC Beams with Regular Web Openings and Non-corroding GFRP Reinforcement. International Journal of Concrete Structures and Materials, 18(1), 77.

Kartal, S., Gündoğan, U., & Kalkan, I. (2025). CTP Boyuna ve Enine Donatılı Betonarme Kirişlerin Kesme Davranışları. Afyon Kocatepe Üniversitesi Fen Ve Mühendislik Bilimleri Dergisi, 25(4), 854-864.

Kartal, S., Kalkan, I., Mertol, H. C., & Baran, E. (2023). Influence of the proportion of FRP to steel reinforcement on the strength and ductility of hybrid RC beams. European Journal of Environmental and Civil Engineering, 27(12), 3546–3565.

Lau, D., & Pam, H. J. (2010). Experimental study of hybrid FRP RC beams. Engineering Structures, 32(12), 3857–3865. https://doi.org/10.1016/j.engstruct.2010.08.028

Leung, H. Y., & Balendran, R. V. (2003). Flexural behaviour of concrete beams internally reinforced with GFRP rods and steel rebars. Structural Survey, 21(4), 146–157. https://doi.org/10.1108/02630800310507159

Müsevitoğlu, A., Sancıoğlu, S., Akın, S. K., İlgün, A., & Kartal, S. (2025). Considering the existing stirrup location: The axial compressive behavior of partially carbon fiber-reinforced-wrapped square columns. Structural Concrete.

Naaman, A. E., & Jeong, S. M. (1995). Structural ductility of concrete beams prestressed with FRP tendons. In L. Taerwe (Ed.), Non-metallic (FRP) reinforcement for concrete structures (pp. 379–386). E&FN Spon.

Pang, L., Qu, W., Zhu, P., & Xu, J. (2016). Design propositions for hybrid FRP-steel RC beams. Journal of Composites for Construction, 20(5), 04015086. https://doi.org/10.1061/(ASCE)CC.1943-5614.0000654

Qin, R., Zhou, A., & Lau, D. (2017). Effect of reinforcement ratio on the flexural performance of hybrid FRP RC beams. Composites Part B: Engineering, 108, 200–209. https://doi.org/10.1016/j.compositesb.2016.09.054

Qu, W., Zhang, X., & Huang, H. (2009). Flexural behavior of concrete beams reinforced with hybrid (GFRP and steel) bars. Journal of Composites for Construction, 13(5), 350–359. https://doi.org/10.1061/(ASCE)CC.1943-5614.0000035

Ruan, X., Lu, C., Xu, K., Xuan, G., & Ni, M. (2020). Flexural behavior and serviceability of concrete beams hybrid-reinforced with GFRP bars and steel bars. Composite Structures, 235, 111772.

Safan, M. A. (2013). Flexural behavior and design of steel-GFRP RC beams. ACI Materials Journal, 110(6), 677-685.

Spadea, G., Swamy, R. N., & Bencardino, F. (2001). Strength and ductility of RC beams repaired with bonded CFRP laminates. Journal of Bridge Engineering, 6(5), 349–355. https://doi.org/10.1061/(ASCE)1084-0702(2001)6:5(349)

Todeschini, C. E., Bianchini, A. C., & Kesler, C. E. (1964). Behavior of concrete columns reinforced with high strength steels. ACI Journal Proceedings, 61(6), 701–716. https://doi.org/10.14359/7803

Vijay, P. V., & GangaRao, H. V. S. (1996). A unified limit state approach using deformability factors in concrete beams reinforced with GFRP bars. In Materials Engineering Conference Proceedings (Vol. 5, pp. 657–665).

Vijay, P. V., & GangaRao, H. V. S. (2001). Bending behavior and deformability of glass fiber-reinforced polymer RC members. ACI Structural Journal, 98(6), 834–842. https://doi.org/10.14359/10750

Yaz, M. (2014). The effect of glass fiber reinforcement on the flexural behavior of RC beams (Master's thesis). Kırıkkale University, Kırıkkale, Turkey.

Zou, P. X. W. (2003). Flexural behavior and deformability of fiber reinforced polymer prestressed concrete beams. Journal of Composites for Construction, 7(4), 275–284. https://doi.org/10.1061/(ASCE)1090-0268(2003)7:4(275)